

CHAPTER 15

VARIATION OF LATTICE PARAMETER 'a' WITH TEMPERATURE

	CONTENTS	PAGES
15.1	Introduction	294
15.2	Experimental	295
15.3	Results and Discussions	296
15.4	Conclusions	299
15.5	References	300
	Captions of the figures	301
	Figures	302

15.1 Introduction

The facility of taking electron diffraction patterns at different temperatures starting from liquid nitrogen temperature to about 1200°K available in our microscope has been used for the study of variation of lattice parameter with temperature. In past such studies were carried out by Mahalawy and Evans¹⁾ in the temperature range of 295° to 1073° K for 2H-MoS₂ and 2H-WSe₂ crystals. They used X-ray diffraction technique for their measurements. It appears from the literature that there is no report on such studies in 2H-TaS₂ crystals. Therefore attempts made by the author to study the variation of

'a' parameter with temperature of these crystals have been described in this chapter.

15.2 Experimental

Thin specimens of $2H-TaS_2$ were obtained by repeated cleavage from a parent crystal by the method outlined in Chapter 11. Philips EM 400 electron microscope operating at 120 kV was used for taking the electron diffraction patterns at different temperatures. Observations at temperatures below the room temperature were taken in a cooling holder whereas for the temperatures above the room temperature a heating holder was used. It was seen that variation in temperature did not have any apparent effect on the magnification. The uncertainty in the determination of temperature on account of the thermocouple current and the heating effect of the electron beam was $\pm 0.5^\circ$ K. The maximum temperature that can be attained in the heating holder is 1273° K but it purely depends upon the material of the grid being used. On the other hand the minimum temperature attainable by the cooling holder is that of liquid nitrogen. For taking the different patterns at different stages the temperature was maintained constant for about five minutes.

Since the microscope has built in facility for recording the camera length, for the different patterns, it was not necessary to determine the camera length of the electron diffraction camera at each stage.

For the measurement of 'a' parameter, the specimens were oriented in the diffraction camera with their c-axis parallel to the incident electron beam. At each temperature the distances between the pair of $2H-TaS_2$ spots were measured and the corresponding 'd' values were computed using the camera constant. It was then a simple procedure to compute a value for the 'a' parameter. Measurements were made using the following diffraction spots, $\{30.0\}$, $\{20.0\}$, $\{10.0\}$, $\{10.0\}$, $\{20.0\}$ and $\{30.0\}$. A diffraction pattern showing the basal section of a $2H-TaS_2$ crystal is shown in Fig. 15.1. The indexing of the various spots is shown in Fig. 15.2. It may be mentioned that in the present study the temperature range used was from 98 to $726^\circ K$.

15.3 Results and Discussions

The measured values of 'a' for $2H-TaS_2$, in the temperature range mentioned are given in Table 15.1. The nature of graph of 'a' versus T is

Table 12.1Lattice parameter variation with temperature

Sr. No.	Temperature $T^{\circ}(\text{K})$	Lattice parameter a (\AA)
1.	98	3.2500
2.	110	3.2520
3.	170	3.2572
4.	206	3.2735
5.	250	3.2840
6.	279	3.2900
7.	293	3.2935
8.	358	3.3081
9.	395	3.3169
10.	462	3.3320
11.	558	3.3582
12.	609	3.3681
13.	667	3.3880
14.	726	3.4410

shown in Fig. 15.3. The curve through the experimental points is non-linear.

The thermal expansion coefficient (α) at different temperatures was determined from the plot of Fig. 15.3. When α is plotted against T, a curve as shown in Fig. 15.4, is obtained. From this curve one is able to note remarkably an anomalous behaviour of α , i.e. α increases quite rapidly at higher temperatures (above 430° K). Lidiard²⁾ is of the opinion that such an anomalous expansion is expected for ionic crystals in the intrinsic range of temperatures. Lawson³⁾ who studied the thermal expansion of silver halides attributed such anomalous behaviour of α to the thermal generation of point defects.

The anomalous expansion of α is useful in evaluating defect formation energy. According to Lidiard²⁾ the presence of defects produces a fractional change in volume, given by

$$\delta = \frac{\Delta V}{V} = A \exp(-E/2KT) \quad \dots (15.1)$$

where A = a constant and

E = formation energy of the defects.

The additional expansion $\Delta\alpha$ due to this change in volume is

$$\Delta\alpha = \frac{1}{V} \frac{d}{dT} (\Delta V) = \frac{A}{2KT^2} \exp(-E/2KT) \quad \dots (15.2)$$

so that

$$T^2(\Delta\alpha) = \frac{A}{2K} \exp(-E/2KT) \quad \dots (15.3)$$

The values of $\Delta\alpha$, corresponding to different temperatures were determined from the plot of Fig. 15.4. These values were used to plot graph of $\ln(T^2\Delta\alpha)$ versus $\frac{1}{T}$, which is obtained as shown in Fig. 15.5. The graph is essentially a straight line and hence a slope can be easily calculated. The defect formation energy derived using this slope is 0.7945 eV.

15.4 Conclusions

The lattice parameter variations of $2H-TaS_2$ crystals have been studied by taking the electron diffraction pattern at different temperatures. Similar type of studies could not be made for

1T-TaS₂ crystals since they undergo different phase transformations in the temperature range used for the present study.

15.5 References

1. Mahalwy, H. L. and Evans, B. L.
J. Appl. Cryst. **9** (1976) 403.
2. Lidiard, A. B.
Handbook Phys. **20** (1957) 246.
3. Lawson, A. W.
Phys. Rev. **72** (1950) 185.

Captions of the figures

- Fig. 15.1 A diffraction pattern showing the basal section of a $2H-TaS_2$ crystal.
- Fig. 15.2 The diffraction pattern shown in Fig. 15.1 as indexed.
- Fig. 15.3 Plot of variation of lattice parameter 'a' with temperature.
- Fig. 15.4 Plot of coefficient of thermal expansion with temperature.
- Fig. 15.5 Plot of $\log [r^2 (\Delta\alpha)]$ versus $\frac{1}{T}$.

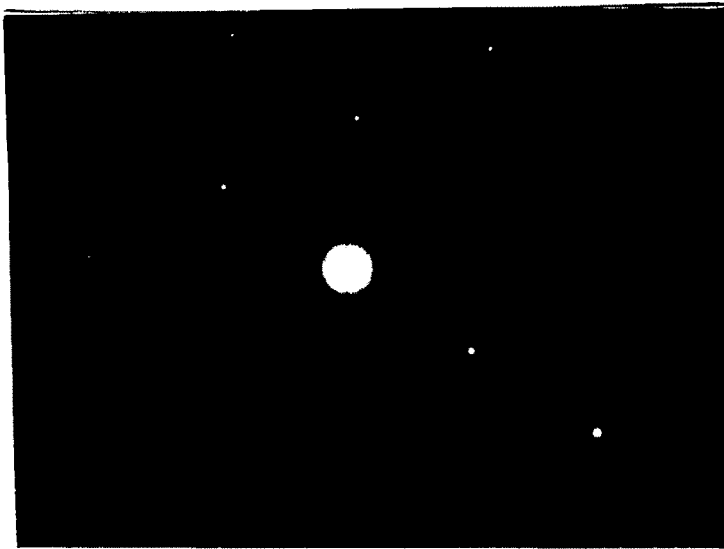


Fig. 15.1

	13.0	03.0	13.0	23.0	33.0	43.0	
	23.0	12.0	02.0	12.0	22.0	32.0	42.0
0	27.0	17.0	07.0	17.0	27.0	37.0	
	30.0	20.0	10.0	00.0	10.0	20.0	30.0
0	31.0	21.0	11.0	01.0	11.0	21.0	31.0
	42.0	32.0	22.0	12.0	02.0	12.0	22.0

Fig. 15.2

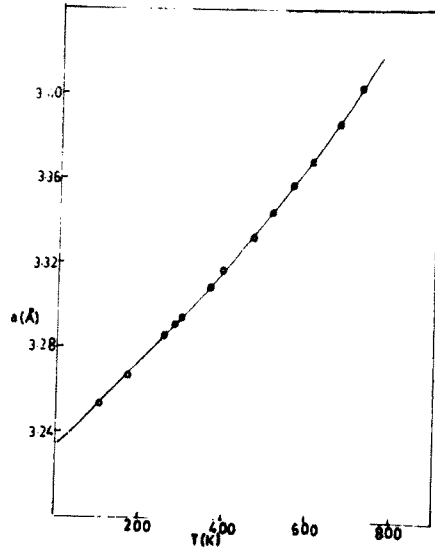


Fig. 15.3

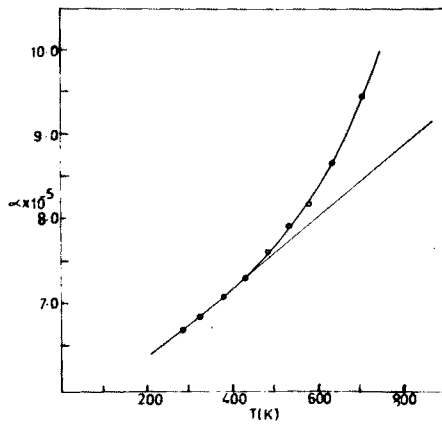


Fig. 15.4

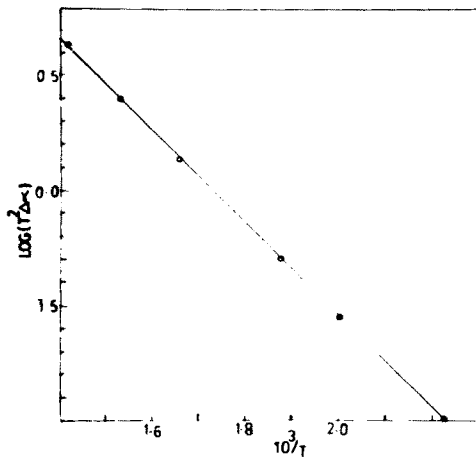


Fig. 15.5